JOURNAL OF MATERIALS SCIENCE 12 (1977) 684–692

Failure of brittle polymers by slow crack growth

Part 3 *Effect of composition upon the fracture of silica particle-filled epoxy resin composites*

R. J. YOUNG
Department of Materials, Queen Mary College, London, UK

P. W. R. BEAUMONT
Department of Engineering, University of Cambridge, Cambridge, UK

The mechanical properties of a silica particle-filled epoxy resin composite system have been investigated in air as a function of volume fraction of particles for volume fractions ranging from 0 to 0.52. The Young's modulus and the compressive yield stress both increase as the volume fraction of silica particles is increased and various models of particle strengthening have been used to explain this behaviour. Slow crack growth in the various particulate composites has been studied using a fracture mechanics approach. The variation of crack velocity (V) with stress intensity factor (K_I) has been measured for each of the compositions investigated. In each case, a unique relationship between V and K_I has been found with K_I increasing with volume fraction of particles at a given value of V. The failure mechanisms and the variation of other fracture mechanics parameters, for example, crack opening displacement and plastic zone size with increasing particle volume fraction have been discussed.

1. Introduction

In the previous paper of this series [1] slow crack growth in an epoxy resin containing about 42% by volume of irregularly shaped silica particles was examined in detail. The variation of crack velocity (V) with stress intensity factor (K_I) was measured using the double torsion (DT) test [2]. A relationship between V and K_I was evaluated using a load relaxation technique that did not require direct observation of the moving crack. It was found that at a given temperature and in a given environment V was a unique function of K_I. At a crack velocity greater than 10^{-5} m sec^{-1} the crack was found to propagate principally through the silica particles and matrix, whereas at velocities below this value the crack tended to go around the particles and fracture occurred by matrix cracking and particle pull-out.

In this paper, $V(K)$ curves have been constructed for other volume fractions of silica particles. The Young's modulus of each particulate composite has been measured as a function of strain-rate; this has enabled us to look at the variation of stress intensity factor (K_I) and the strain energy release rate (G_I), as a function of particle volume fraction, for a given crack velocity. The composites were found to yield and flow in uniaxial compressive loading and the compressive stress–strain relationships have been determined as a function of the volume fraction of silica particles. This has enabled other fracture mechanics parameters such as crack opening displacement and plastic zone size for different amounts of silica particles to be determined.

2. Experimental

2.1. Materials and test conditions

A series of epoxy resin composites containing up to 52 vol % silica particles were studied. They were supplied by Ciba-Geigy (UK) Ltd, (Duxford) in

TABLE I Volume fraction V_p of silica particles and interparticle spacing d in the composite

	x						
	0	50	100	150	200	250	300
V_p	0	0.15	0.26	0.35	0.42	0.47	0.52
$d(\mu m)$	∞	262	131	87	63	52	46

x is the number of parts by weight of silica in the resin. The specific gravity of the resin has been taken as 1.23 and that of the silica as 2.65 [1]. d has been calculated from Equation 9.

the form of cast plates approximately 6 mm thick. The resin (CT200), hardener (HT901) and silica flour (Z300) have been described in a previous publication [1]. The ratio of resin : hardener : filler was 100 : 30 : x parts by weight where x varied in increments of 50 from 0 to 300. All the samples had been cured at 135° C for 16 h. The composition of each composite is given in Table I. Optical micrographs of the microstructures of some of the composites are shown in Fig. 1. The irregular shape and size variation of the silica particles can be seen. The appearance of the micrographs are consistent with a sieve analysis of the particles [1] which showed that over 50% of the particles were in the size range of 64 to 74 μm.

All the mechanical testing was carried out at 20 ± 2° C in air at r.h. 60 ± 10%.

2.2. Young's modulus determinations

The Young's modulus, E, of each composite was determined as a function of cross-head speed using a three-point bend test performed in an Instron mechanical testing machine. The relationship between the applied load, P, and the displacement at the centre of the specimen, y, is given by

$$P = \frac{4Ebh^3}{L^3} y \qquad (1)$$

for specimens of rectangular cross-section (of thickness h and breadth b). L is the distance between the supports. The Young's modulus, E, was determined from the slope of a plot of P against y and the specimen dimensions. The plot was linear over the range of strain investigated (up to 0.005). An average strain-rate, $\dot{e}$, in the specimen was estimated from the cross-head speed and specimen dimensions. It was taken as the strain-rate at a

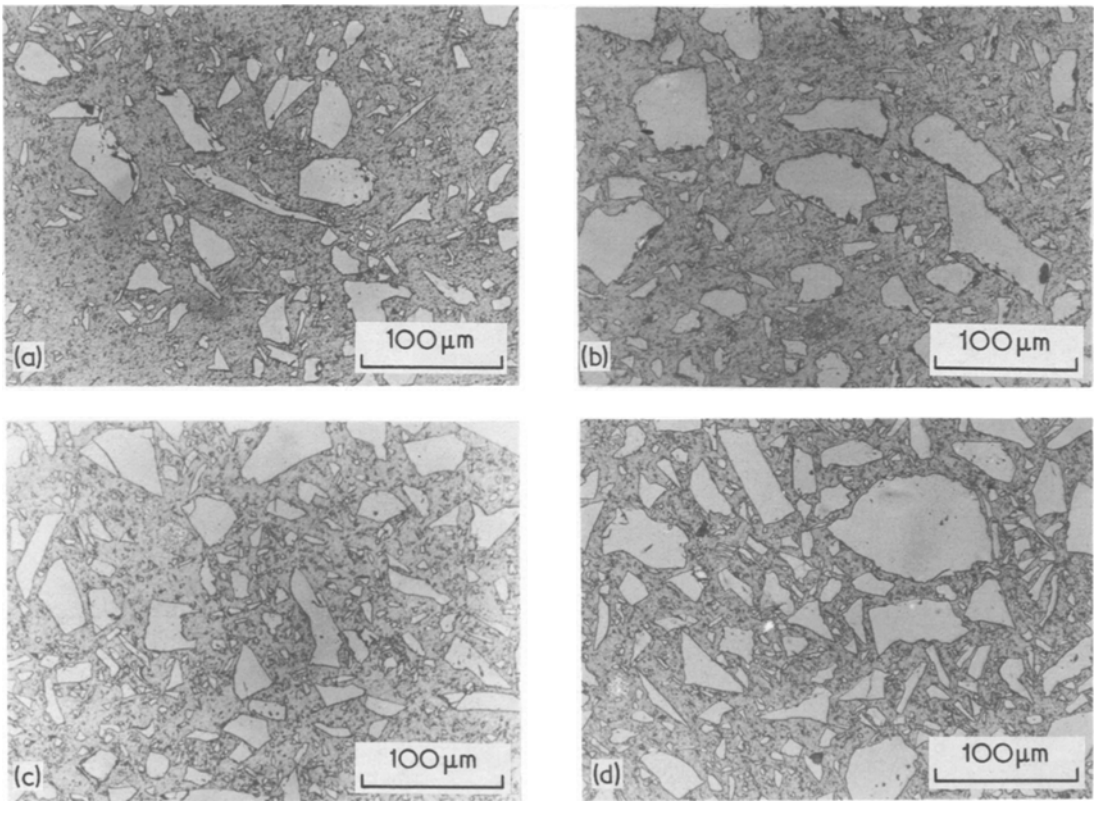

Figure 1 Optical micrographs of polished sections of samples of the composite with different volume fractions of particles. (a) 0.26 (b) 0.35 (c) 0.42 (d) 0.47.

point half-way between the neutral axis and the specimen surface.

2.3. Measurement of stress–strain curve

Rectangular specimens 10 mm long and with a 5 mm square cross-section were machined from the cast plates. They were deformed in uniaxial compression between polished steel dies lubricated with a molybdenum disulphide based grease. A cross-head speed of 0.5 mm min^{-1} was used which is equivalent to an initial strain-rate of 8×10^{-4} sec^{-1}. The strain was calculated from the displacement of the cross-head and the initial specimen height. The true stress on the specimen was calculated from the applied load, the initial cross-sectional area of the specimen and the strain by assuming that deformation took place at constant volume. This assumption will lead to a small error in true stress at the low strains used (< 0.15).

2.4. Double torsion tests

Crack propagation in the various composites was investigated using the double torsion (DT) test which enabled a rapid determination of crack velocity (V) as a function of stress intensity factor (K_I).

2.4.1. Specimen design and analysis

The design and analysis of the DT specimen has been described in detail elsewhere [2]. K_I is independent of crack length and for an elastic material is given by

$$K_I = PW_m \left[\frac{3(1+\nu)}{Wt^3 t_n}\right]^{1/2} \quad (2)$$

where $W/2 \gg t$. P is the applied load, W_m is the moment arm, ν is Poissons ratio of the material, W is the bar width, t is the plate thickness and t_n is the thickness of the plate in the plane of the crack. This analysis assumes that the specimen is made up of two thin plates of width $W/2$ which are both strained in torsion. However, it has been pointed out to us [3] that only when $(W/2)/t$ is greater than 10 can Equation 2 be used with any accuracy. When $W/2 < 10$ a systematic error is introduced and K_I is underestimated. Using an analysis of Timoshenko and Goodier [4] to describe the torsion of a beam Equation 1 is rewritten as

$$K_I = PW_m \left[\frac{1+\nu}{Wt^3 t_n k_1}\right]^{1/2} \quad (3)$$

TABLE II Variation of k_1 with $(W/2)/t$ [4] and the error in K_I introduced by having a double torsion specimen of finite width

	$(W/2)/t$					
	1	1.5	2.5	4	10	∞
k_1	0.146	0.196	0.249	0.281	0.312	0.333
Error (%)	53.9	30.4	15.7	8.9	3.4	0

where k_1 is a constant which depends on the ratio $(W/2)/t$. The variation of k_1 with $(W/2)/t$ is given in Table II (NB $k_1 = 1/3$ when $(W/2)/t = \infty$). For specimens used in the present investigation, $(W/2)/t$ was of the order of 2.5 and K_I has been calculated using Equation 3.

2.4.2. Measurement of crack velocity

For specimens which exhibited continuous crack growth, the crack velocity was estimated using the methods described earlier [1, 2]. They included direct crack observation, load relaxation and constant cross-head displacement-rate techniques.

When specimens underwent crack jumping, the crack velocity was estimated using a modification of the load relaxation method, described by Phillips and Scott [5].

In all cases a correction factor was used to take into account the curved profile of the crack front [1, 2].

3. Results and discussion

3.1. Young's modulus

The variation of modulus with strain-rate for each of the composites is given in Fig. 2. It can be seen

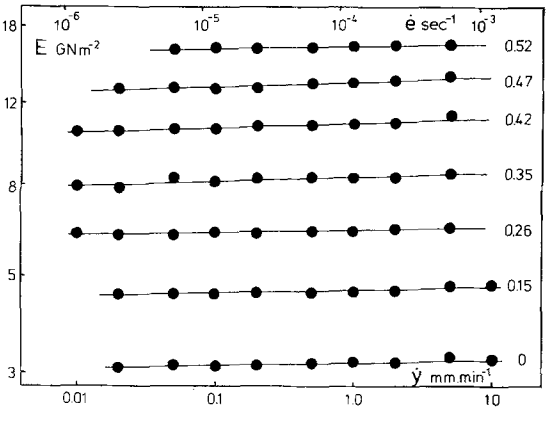

Figure 2 Variation of the Young's modulus of the composite, measured in bending, with cross-head speed and strain-rate. Each curve corresponds to a different volume fraction of particles.

that the modulus increases significantly with volume fraction of particles and increases only slightly with loading rate. Fig. 3 shows the variation of modulus with particle volume fraction for a particular strain-rate (10^{-4} sec^{-1}). The broken

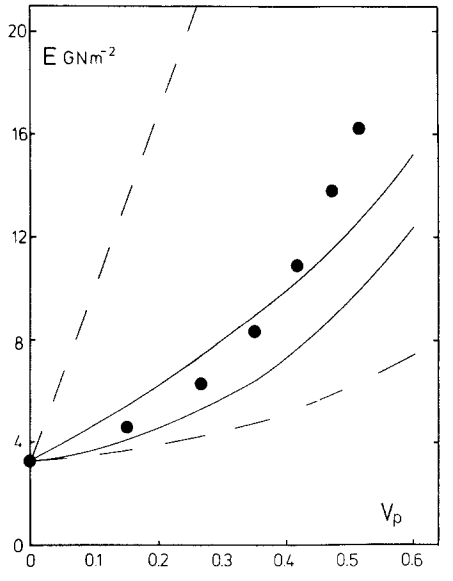

Figure 3 Variation of the Young's modulus of the composite with volume fraction of particles V_p measured at a strain-rate of 10^{-4} sec^{-1}. The two broken lines are from Equations 4 and 5 and the continuous lines from Equations 6 and 7 respectively.

curves in this figure are the predicted upper and lower bounds of modulus of a particulate composite using a model due to Paul [6] and based upon strain energy theorems. The upper bound is given by

$$E_c = E_p E_m / [(1 - V_p)E_p + V_p E_m] \quad (4)$$

and assumes that the particles and matrix are equally stressed. E_c, E_m and E_p are the values of Young's modulus of the composite, matrix and particles respectively and V_p is the volume fraction of the particles. The lower bound is given by the simple rule of mixtures equation:

$$E_c = (1 - V_p)E_m + V_p E_p \quad (5)$$

E_m has been taken to be 3.16 GN m^{-2} and E_p to be 73.1 GN m^{-2} [7]. The two bounds are widely spaced and the experimental points lie well within them.

A better theoretical estimate can be obtained using the equations of Ishai and Cohen [8] which are based on the work of Paul [6]. The model is that of a cubic particle surrounded by a cube of matrix. The upper bound of E_c which in this case is for a uniform stress applied at the boundary of the cube, is given by

$$E_c = E_m \left[\frac{1 + (m-1)V_p^{2/3}}{1 + (m-1)(V_p^{2/3} - V_p)} \right] \quad (6)$$

where m is equal to E_p/E_m. The lower bound is found using the same model [8] and is for uniform displacement at the boundary. It is given by

$$E_c = E_m \left\{ 1 + \frac{V_p}{[m(m-1) - V_p^{1/3}]} \right\}. \quad (7)$$

The bounds given by Equations 6 and 7 are much closer together and they are drawn as solid lines in Fig. 3. The experimental points lie between these bounds up to a particle volume fraction of 0.4 but they tend to rise above the upper bound at higher volume fractions. Particle strengthening of an epoxy resin has been observed by Ishai and Cohen [8] in tension and compression. The deviation from the theoretical prediction at high volume fractions observed by Ishai and Cohen [8] and ourselves, is probably due to the particles becoming in contact with one another and without a continuous layer of matrix between them.

Radford [9] has fitted the modulus particle volume fraction data of similar particulate com-

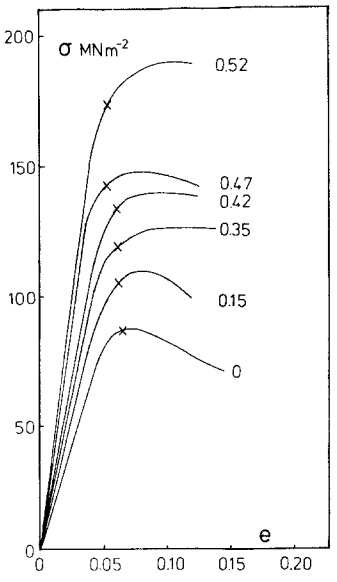

Figure 4 True stress versus nominal strain measured in compression at an initial strain rate of 8×10^{-4} sec^{-1} for samples of the composite. A 1% offset yield stress is marked upon each of the curves.

posites to an empirical equation. The data obtained in this investigation for any given strain-rate may be fitted to a similar equation. In this case the Young's modulus is given by

$$E_c = E_m(1 - V_p)^{-7/3}. \quad (8)$$

Although the data fit the equation very accurately, the physical significance is unclear.

3.2. Stress–strain behaviour

Stress–strain curves for each of the composites are given in Fig. 4. All the samples yielded and flowed in uniaxial compression in contrast to their brittle nature in tension. The pure epoxy resin and composites having low values of V_p were able to flow to over 30% plastic strain before cracking. This ability to undergo plastic flow decreased as V_p was increased and for the highest particle volume fraction studied ($V_p = 0.52$) fracture occurred soon after the specimen had reached the maximum load. All the silica-filled composites were seen to stress-whiten after yield. Fig. 5 shows a pair of optical micrographs of sections of specimens with V_p equal to 0.52. The surface of an undeformed specimen is shown in Fig. 5a and that of a deformed specimen is shown in Fig. 5b. It can be seen that after deformation the specimen contains many particles with cracks parallel to the compression direction. The cracks may be caused by tensile strains perpendicular to the compression direction induced by the compressive stress.

The yield point for these composite materials is difficult to define. In the stress–strain curves which show a drop in true stress after yield, the maximum stress can be taken as the yield stress. However, all the curves do not show a load drop and a 1% off-set stress has been taken to define the yield stress.

For a given size of particle, the average separation between particles decreases as the value of V_p is increased. The inter-particle spacing, d, can be estimated from the equation [10]

$$d = \frac{2D(1 - V_p)}{3V_p}, \quad (9)$$

where D is the average particle size. The yield stress of each of the composites is plotted against the reciprocal of the average inter-particle spacing in Fig. 6. The points are scattered but it does appear that the yield stress of the composite σ_{yc} can be described by an equation of the form

$$\sigma_{yc} = \sigma_{ym} + \frac{S}{d} \quad (10)$$

where σ_{ym} is the yield stress of the matrix and S is a constant that is equal to 3.4×10^{-3} MN m^{-1}. A relationship similar to the one described in Equation 10 has been successful in estimating the yield stress of precipitation hardened metals [11].

Some preliminary experiments have also been

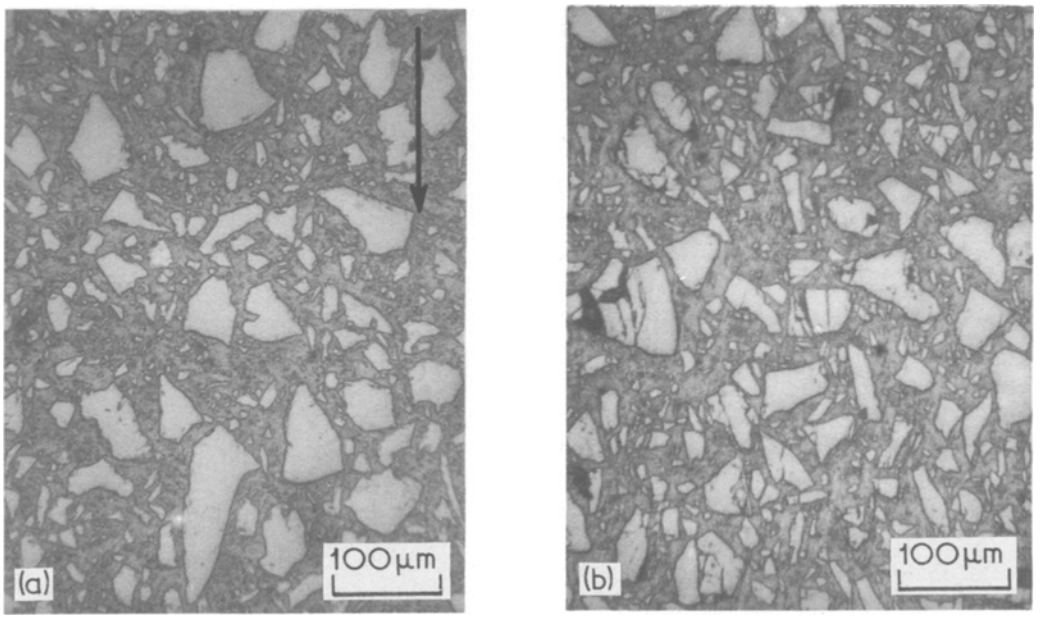

Figure 5 Optical micrographs of polished sections of the composite material containing 0.52 by volume of silica particles: (a) undeformed; (b) after being taken to a compressive strain of 0.12. Arrow indicates compression direction.

carried out to study the effect of strain-rate upon the yield stress of these composites. The stress–strain data given here are subject to a scatter of ± 5%, but it does appear that the yield stress increases with strain-rate.

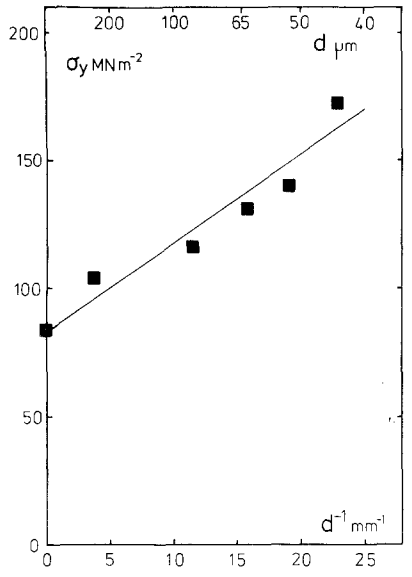

Figure 6 Yield stress as a function of the reciprocal of the interparticle spacing in the composite (Table I).

3.3. $V(K)$ measurements

The curves showing the relationships between V and K_I for pure epoxy resin and silica–epoxy composites are given in Fig. 7. The experimental points have been omitted although $V(K)$ curves with experimental points have been published for the pure resin [12] and composite containing 42% silica [1]. The amount of scatter of data obtained in this earlier work is typical of that found in the present investigation. The curves have been plotted between crack velocities of 10^{-8} and 10^{-2} m sec^{-1}. Data over this range of velocity were not obtained for all samples and in these cases the curves have been extrapolated to cover the full range of crack velocity. It can be seen in Fig. 7 that the value of K_I associated with a particular crack velocity increases with the volume fraction of silica particles. Crack jumping tended to occur in the DT specimens containing lower volume fractions of silica (0 and 0.15). In contrast, crack propagation occurred in a more continuous stable manner with higher volume fractions of particles.

4. Crack propagation

4.1. Fracture energy

From a fracture mechanics point of view, crack propagation in the composite becomes more difficult as the volume fraction of silica particles is increased. However, a rather different picture emerges when the fracture energy is considered. The strain energy release rate G_I is related to both K_I and E and is given [13] approximately by the equation

$$G_I \sim K_I^2/E. \qquad (11)$$

The exact value of G_I will depend upon the crack velocity at which K_I was determined and the strain-rate at which E was measured. The crack velocity and strain-rate should be related [14] but the relationship between the two depends upon the nature of the plastic zone at the tip of the crack. A strain-rate of 10^{-4} sec^{-1} and a crack velocity of 10^{-5} m sec^{-1} have, therefore, been chosen arbitrarily. The value of $G_I(K_I^2/E)$ calculated from Equation 11 has been given for each specimen in Table III. In contrast to K_I, G_I reaches a maximum at a volume fraction of about 0.3 and then falls off. This is because the modulus E increases with volume fraction at a faster rate than the increase in K_I^2.

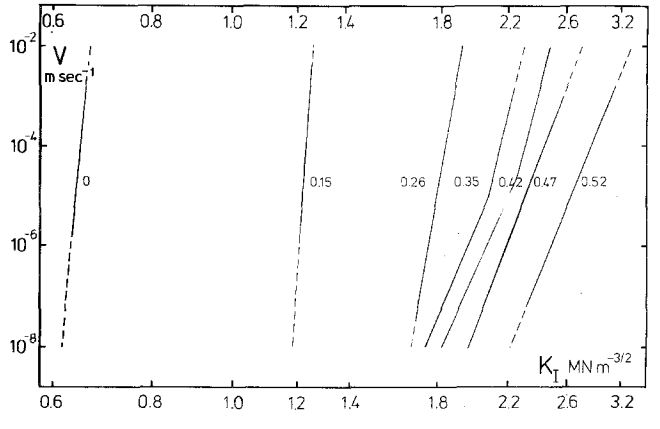

Figure 7 Crack velocity (V) as a function of stress intensity factor (K_I) for the composites tested in air. Data points have been obtained for the continuous lines. The broken lines are extrapolations of the continuous lines where no data points are available.

TABLE III The variation of σ_y, K_I, E and K_I^2/E with volume fraction of particles in the composite V_p

V_p	σ_y (MN m^{-2})	K_I (MN m$^{-3/2}$)	E (GN m^{-2})	K_I^2/E (J m^{-2})
0	84	0.644	3.16	131.2
0.15	104	1.228	4.62	326.4
0.26	109*	1.800	6.31	513.5
0.35	116	2.089	8.32	524.5
0.42	131	2.203	10.96	442.8
0.47	140	2.317	13.80	389.0
0.52	172	2.636	16.25	427.6

σ_y has been determined at a strain-rate of 8×10^{-4} sec^{-1}, K_I is given for a crack velocity of 10^{-5} m sec^{-1} and E is given for a strain-rate of 10^{-4} sec^{-1}.
*Extrapolated value.

It has been suggested that the fracture energy of brittle materials reinforced with brittle second phase particles may increase as the inter-particle distance is decreased due to a line energy effect associated with crack-front particle interaction [15]. Equation 9 shows that the inter-particle spacing will decrease as the volume fraction of particles is increased. Lange [15] suggested that the relationship between G_I and d would be of the form

$$G_I^c = G_I^o + \frac{T}{d}, \qquad (12)$$

where G_I^o is the strain energy release rate of the pure resin and G_I^c is the strain energy release rate of the composite with an inter-particle spacing of d. T is the line energy of the crack front. Fig. 8 is a plot of K_I^2/E against $1/d$ for the various composites tested. K_I^2/E increases linearly as the inter-particle spacing is reduced, until about 150 μm, ($V_p \approx 0.25$) as implied by Equation 12 giving a value of T of 0.05 J m^{-1}. At spacings below this value the equation no longer holds and a further increase in K_I^2/E (or G_I) that is predicted does not occur. The reason for this is unclear. There is some evidence that in epoxy composite systems the mode of fracture may change as the particles become too close for an effective crack front interaction [10]. It is known that the mode of fracture in these materials may change with crack velocity also [1]. The mechanisms of failure in these materials have been discussed in detail in a previous publication [1], and this is clearly an area where more investigations are needed.

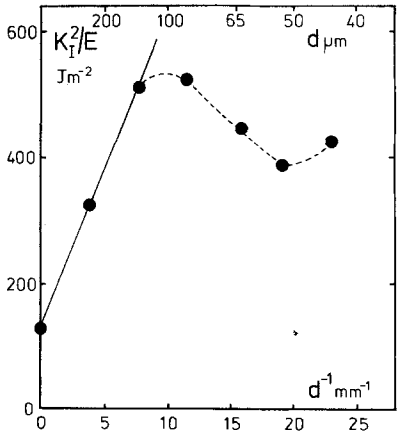

Figure 8 K_I^2/E or G_I as a function of the reciprocal of the interparticle spacing (Table I).

This maximum in G_I at a critical value of d (or $1/d$) may be accounted for by an alternative explanation. If the formation of a crack in a particulate composite requires a critical amount of stored elastic strain energy within the particles and the surrounding matrix, (as suggested by Davidge and Green [17]), then this pre-requisite for cracking must, therefore, be dependent upon V_p. Davidge and Green showed that for thoria spheres in a glass matrix most of the stored elastic strain energy in the matrix was in a shell of thickness $D/2$ around the particles. Since one assumption of their model is that the strain energy field of an individual particle is not interfered with by an overlapping field, then for this to happen the interparticle separation d must be equal to greater than the particle diameter D. For our silica particle epoxy resin composites this would correspond to an inter-particle separation of 70 μm. The maximum in the plot of G_I against $1/d$ occurs at a value of d of the order of 100 μm ($V_p \sim 0.3$) and so it may be that at high values of V_p the strain fields overlap and there is no further particle toughening.

One important point to note for failure-safe design purposes is that it is the value of K_I that is important rather than that of G_I. The fracture stress σ_f of a specimen containing a small flaw or crack of length a may be given by a Griffith type relationship such as

$$\sigma_f \sim \left(\frac{G_{IC}E}{\pi a}\right)^{1/2} \sim \frac{K_{IC}}{\sqrt{(\pi a)}}, \qquad (13)$$

where G_{IC} and K_{IC} are the values of G_I and K_I required to produce catastrophic failure. This means for a given crack length or flaw size the fracture stress will be higher if K_{IC} is higher for that material. The value of fracture stress will also depend upon the product of G_{IC} and E. Anything which increases or decreases G_{IC} may

also change E and so changes in both of these parameters must be considered for predictions of fracture stress.

4.2. Plastic zone

In the absence of any direct observations of the crack tip during crack propagation this section can only be speculative. However, enough information has been obtained to enable the crack opening displacement and plastic zone size to be determined if the plastic zone at the tip of the crack is assumed to be of a certain geometry.

It has been shown [14] that in polymers such as PMMA the plastic zone at the tip of the crack may be modelled successfully as a Dugdale line plastic zone. In this case the length R of the plastic zone is given by [14]

$$R = \frac{\pi}{8}\left(\frac{K_I}{\sigma_y}\right)^2 \tag{14}$$

and the crack opening displacement δ_t is given by [14]

$$\delta_t = \frac{K_I^2}{\sigma_y E}. \tag{15}$$

The values of R and δ_t have been calculated using the experimentally determined values of K_I, E and σ_y (from Table III) and are given in Fig. 9 as a function of volume fraction. The exact values of R and δ_t will depend upon the crack velocity and strain-rate chosen. However, both R and δ_t increase at first and then reach a maximum at a particle volume fraction of the order of 0.3. There is no evidence that in epoxy resins or epoxy resin composites that the plastic zone is of the Dugdale type. Indeed if the plastic zone in the pure resin were a craze of length 23 μm as the Dugdale model implies, it would certainly be visible to the naked eye which does not appear to be the case. Also it is difficult to define what is meant by a plastic zone in a composite material and it is also likely that the geometry of any plastic zone might change as the volume fraction of particles is altered.

If the material contains a plane strain plastic zone the values of R and δ_t can again be calculated. In this case they are given by [16]

$$R = \frac{1}{3\pi}\left(\frac{K_I}{\sigma_y}\right)^2 \tag{16}$$

and

$$\delta_t \sim 0.5\,\frac{K_I^2}{\sigma_y E}, \tag{17}$$

and are smaller than the values given by the Dugdale model. However, they differ from the Dugdale values by a constant factor and are given by the right-hand ordinate in Fig. 9. The maxima in R and δ_t at a volume fraction of 0.3 are consistent with the maximum in G_I (K_I^2/E) at a similar composition.

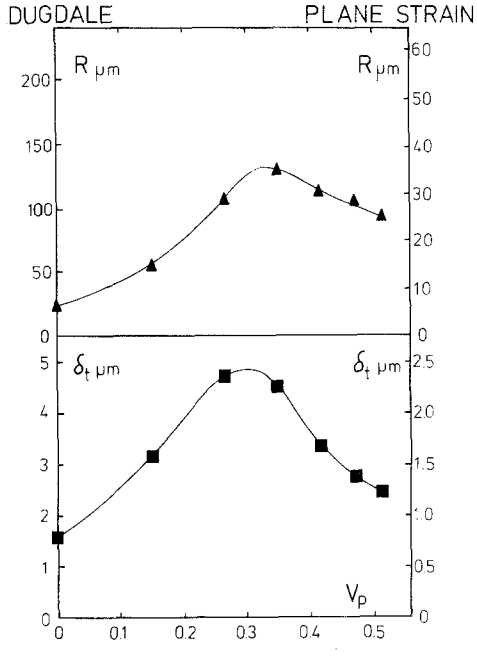

Figure 9 Plastic zone size (R) and crack opening displacements (δ_t) as a function of the volume fraction of particles V_p. The axis in the left-hand side refers to the values given by the Dugdale model and the axis on the right-hand side is for the values obtained for a plane strain plastic zone.

5. Conclusions

It has been shown that the addition of silica particle to an epoxy resin can have a profound effect upon the mechanical properties. The Young's modulus measured in bending and the yield stress measured in compression are both increased. It has been found that under identical experimental conditions for each of the composites investigated the crack velocity (V) is a unique function of the stress intensity factory (K_I) and for a given crack velocity the stress intensity factor increases markedly with the volume fraction of the second phase particles.

Various other fracture mechanics parameters have been calculated for the system. It is found that the strain energy release rate (G_I), crack opening displacement (δ_t) and plastic zone size

(R) increase at first with increasing volume fraction of particles. They all reach a maximum at a volume fraction of about 0.3 and then decrease at higher volume fractions. However, the volume fraction that gives these maxima cannot be said to be the optimum composition. The fraction stress varies with inherent flaw size and is dependent upon K_I rather than any of these other fracture mechanics parameters. For complete knowledge of the failure behaviour of these materials the crack initiation processes and variation of inherent flaw size with composition would have to be evaluated.

Acknowledgements

We are grateful to Mr Graham Hodgetts of CIBA–GEIGY (UK) Limited (Duxford) for providing us with moulded plates of the composite and to Mr T. W. Wong for obtaining some of the stress–strain data. Part of this work was supported by the Science Research Council.

References

1. R. J. YOUNG and P. W. R. BEAUMONT, *J. Mater. Sci.* **10** (1975) 1343.
2. *Idem, ibid* **10** (1975) 1334.
3. G. P. MORGAN, University of Leeds, private communication.
4. S. TIMOSHENKO and J. N. GOODIER, "Theory of Elasticity", 2nd Edn. (McGraw-Hill, New York, 1951).
5. D. C. PHILLIPS and J. M. SCOTT, *J. Mater. Sci.* **9** (1974) 1202.
6. B. PAUL, *Trans. Met. Soc. AIME* **218** (1960) 36.
7. G. W. C. KAYE and T. H. LABY, "Tables of Physical and Chemical constants", 13th Edn (Longmans, London, 1966).
8. O. ISHAI and L. J. COHEN, *Int. J. Mech. Sci.* **9** (1967) 539.
9. K. C. RADFORD, *J. Mater. Sci.* **6** (1971) 1286.
10. F. F. LANGE and K. C. RADFORD, *ibid* **6** (1971) 1197.
11. R. W. K. HONEYCOMBE, "The Plastic Deformation of Metals" (Edward Arnold, London, 1968).
12. R. J. YOUNG and P. W. R. BEAUMONT, *J. Mater. Sci.* **11** (1976) 776.
13. J. F. KNOTT, "Fundamentals of Fracture Mechanics" (Butterworths, London, 1973).
14. G. P. MARSHALL, L. H. COUTTS and J. G. WILLIAMS, *J. Mater. Sci.* **9** (1974) 1409.
15. F. F. LANGE, *Phil. Mag.* **22** (1970) 983.
16. A. S. TETELMAN and A. J. McEVILY, "Fracture of Structural Materials", (John Wiley, New York, 1967).
17. R. W. DAVIDGE and T. J. GREEN, *J. Mater. Sci.* **3** (1968) 629.

Received 9 July and accepted 27 July 1976.